SUBBAND ACTIVE NOISE CONTROL ALGORITHM BASED ON A DELAYLESS SUBBAND ADAPTIVE FILTER ARCHITECTURE

Jeong-Hyeon Yun[1,2] *Young-Cheol Park*[3] *Dae-Hee Youn*[1]

[1]ASSP Lab., Dept. of Electronic Eng., Yonsei University
134 Shinchon-Dong, Sudaemoon-Ku, Seoul, 120-749, Korea
[2]LG Industrial Systems Co., Ltd.
533 Hogae-Dong, Dongan-Gu, Anyang-Shi, Kyongki-Do, 430-080, Korea
[3]Samsung Electronic Co., Ltd., Semiconductor MICRO
San #24 Nongseo-Ri, Kiheung-Eup, Yongin-Shi, Kyongki-Do, 449-900, Korea

ABSTRACT

In this paper, a new active noise control algorithm based on a delayless subband adaptive filter architecture is presented. Also, an on-line system identification method implemented in the subband structure is suggested. To implement the filtered-x LMS algorithm in the subband structure, the secondary path transfer function is decomposed into sets of subband functions. The two filter on-line modeling algorithm is then applied to each subband to estimate the secondary-path transfer function in a decomposed form. In this manner, the computational load for the on-line system identification is reduced by a factor 3 compared with the wideband approach. Simulation results are presented to show the efficiency of the new ANC algorithm and the performance of the on-line system identification scheme.

1. INTRODUCTION

Wideband active noise control (ANC) requires several hundred taps to realize significant cancellation of disturbances [1]. In addition to computational complexity, adaptive filters with many taps suffer from slow convergence, especially, if the eigenvalues of the underlying correlation matrix of the input signal are widely spread [2].

Recently, subband techniques have been developed for adaptive filters [3] to reduce computational complexity and to improve the convergence speed of the algorithm. However, a disadvantage of such a subband adaptive filter is that delay is introduced into the signal path by virtue of the bandpass filters used to derive the subband signals. For active noise control, delay is a factor that seriously limits the bandwidth over which good cancellation can be achieved. The delayless subband adaptive filter architecture was suggested by Morgan [4], in which the adaptive weights are computed in subbands, but collectively transformed into an equivalent set of wideband filter coefficients. In such a way, signal path delay is avoided while retaining the computational and convergence speed advantages of subband processing. An additional benefit accrues through a significant reduction of aliasing effects.

For the adaptive filter to properly converge to a desired solution in the process of active noise control, it is necessary to compensate for the distortion caused by the secondary path. Therefore, a modified version of the LMS algorithm, the filtered-x LMS (FXLMS) algorithm was developed [5, 6].

In this paper, a new active noise control algorithm based on a delayless subband adaptive filter architecture [4] is presented. Morgan suggested an ANC algorithm adopting the delayless subband structure [4], in which the secondary path distortion is compensated by filtering the reference input with an wideband filter modeling the secondary path. In the new ANC algorithm, the secondary path transfer function is decomposed into sets of subband functions to implement the filtered-x LMS algorithm. The filtered reference inputs are then generated for each subband by using finite impulse response (FIR) filters that model the secondary path transfer function corresponding to each of subband.

The secondary path can be estimated off-line, prior to operation of the ANC system. However, for some applications the secondary path may be time-varying. In that case it is desirable to estimate the secondary path on-line when the ANC is in operation, in order to assure the stability and convergence of the adaptive filter. To identify the impulse response of the secondary path during real-time operation, an on-line system identification method implemented in the subband structure is also suggested in this paper. Since the secondary path transfer function is adaptively estimated for each subband, the structure presented here has benefits in computational complexity. It is shown that the computational load required to estimate the secondary path transfer function in on-line is reduced by a factor 3 in the new structure compared with the wideband approach.

Computer simulations are performed to evaluate the efficiency of the ANC algorithm and the on-line system identification scheme presented here.

2. DELAYLESS SUBBAND ACTIVE NOISE CONTROL ALGORITHM WITH ON-LINE SYSTEM IDENTIFICATION FILTER

The delayless subband ANC algorithm [4] assumes off-line modeling of the secondary path. In some ANC problems, due to constant changes of the secondary path, it is necessary to identify the impulse response of the secondary path during the real-time operation in order to assure the stability and convergence of the adaptive filter. The delayless subband ANC system combined with the on-line system identification filter is presented in Fig. 1. The polyphase FFT technique is often employed to generate subband input signals. This technique realizes M contiguous single-sideband bandpass filters whose outputs are downsampled by a factor $D = M/2$ to

This work is supported by the Korea Science and Engineering Foundation.

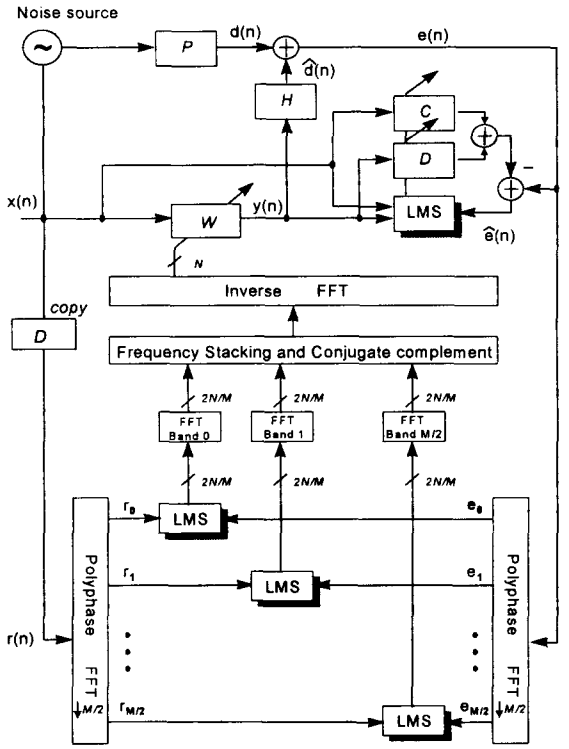

Fig. 1. Delayless subband ANC system combined with the on-line system identification filter.

produce M complex subband signals. In this paper, the $2\times$ oversampled polyphase FFT subband filtering technique [7] is utilized.

The block P in Fig. 1 represents the transfer function from the noise source to the error sensor, and H denotes the transfer function from the adaptive filter output to the error sensor. Let $x(n), x(n-1), \ldots, x(n-N+1)$, and $w_0(n), w_1(n), \ldots, w_{N-1}(n)$ represent reference input samples and tap coefficients of the Nth order adaptive filter at time instant n, respectively. Assuming the secondary path transfer function between the filter output and the output of the error sensor is modeled as an Lth order FIR filter, the error signal $e(n)$ and the filtered reference signal $r(n)$ can be expressed as

$$e(n) = d(n) + \mathbf{w}^T(n)\mathbf{r}(n), n = 0, 1, 2, \ldots, \quad (1)$$

where

$$\mathbf{r}(n) = [r(n), r(n-1), \ldots, r(n-N-1)]^T, \quad (2)$$

and

$$r(n) = \sum_{l=0}^{L-1} d_l(n)x(n-l), n = 0, 1, 2, \ldots \quad (3)$$

As described in [4], the filtered reference signal $r(n)$ and the error signal $e(n)$ are decomposed into sets of subband signals. In each subband, the signals are decimated by a factor of D and the subband adaptive weights are computed by the complex normalized LMS (NLMS) algorithm [8]. The adaptive weights in each subband are then transformed into frequency domain using DFT, appropriately stacked, and inverse transformed to obtain the wideband filter coefficients. For real signals, the wideband filter coefficients are real and only half of the subbands need to be processed, corresponding to the positive frequency components of the wideband filter response. The other half of the response is formed in complex conjugate symmetry.

For N wideband adaptive weights, there are N/D adaptive weights for each subband. The update of the subband adaptive filter weights is expressed for each subband as

$$\mathbf{w}_m(n+D) = \mathbf{w}_m(n) + \frac{\mu}{\sigma_r^2(n)}\mathbf{r}_m^*(n)e_m(n), m = 0, 1, \ldots, M-1, \quad (4)$$

$$\sigma_r^2(n) = (1-\mu)\sigma_r^2(n-1) + \mu r^2(n), \quad (5)$$

where $\mathbf{w}_m$ is a vector of N/D subband weights, $\mathbf{r}_m$ is a vector of filtered reference signal with superscript $*$ denoting complex conjugate, and $e_m(n)$ is the error signal. An IIR recursion is employed to estimate the power of the reference input $\sigma_r^2(n)$.

For on-line identification of the secondary path, the approach presented in [9] is utilized. Define the coefficient vectors of the Lth order system identification filter as

$$\mathbf{c}(n) = [c_0(n), c_1(n), \ldots, c_{L-1}(n)]^T, \quad (6)$$

$$\mathbf{d}(n) = [d_0(n), d_1(n), \ldots, d_{L-1}(n)]^T. \quad (7)$$

Here, $\mathbf{c}(n)$ represents an estimate of the primary path (P in Fig. 1), and $\mathbf{d}(n)$ represents an estimate of the secondary path (H in Fig. 1). The weight vectors $\mathbf{c}(n)$ and $\mathbf{d}(n)$ are updated to minimize the power of the error signal, defined as $\hat{e}(n)$. Therefore, $\hat{e}(n)$ is given by

$$\hat{e}(n) = e(n) - \mathbf{c}^T(n)\mathbf{x}(n) - \mathbf{d}^T(n)\mathbf{y}(n), \quad (8)$$

where $\mathbf{y}(n)$ is an output of wideband adaptive filter defined as

$$\mathbf{y}(n) = [y(n), y(n-1), \ldots, y(n-L-1)]^T. \quad (9)$$

The weight vector can be updated using the NLMS algorithm. Consequently, a dual channel version of the NLMS updates for the system identification filter is given by

$$\mathbf{c}(n+1) = \mathbf{c}(n) + \frac{\kappa}{\sigma_x^2(n) + \sigma_y^2(n)}\hat{e}(n)\mathbf{x}(n), \quad (10)$$

$$\mathbf{d}(n+1) = \mathbf{d}(n) + \frac{\kappa}{\sigma_x^2(n) + \sigma_y^2(k)}\hat{e}(n)\mathbf{y}(n), \quad (11)$$

$$\sigma_x^2(n) = (1-\kappa)\sigma_x^2(n-1) + \kappa x^2(n), \quad (12)$$

$$\sigma_y^2(n) = (1-\kappa)\sigma_y^2(n-1) + \kappa y^2(n). \quad (13)$$

Here, the adaptation constant κ should satisfy the condition $0 < \kappa < \frac{2}{L+1}$ for convergence [9].

3. SUBBAND-DECOMPOSED SECONDARY PATH TRANSFER FUNCTION

The filtered reference signal is obtained by filtering the reference signal by the secondary path transfer function estimate. Instead of generating the filtered reference signal through filtering over the entire band of interest, the secondary path transfer function can be decomposed into sets of subband functions.

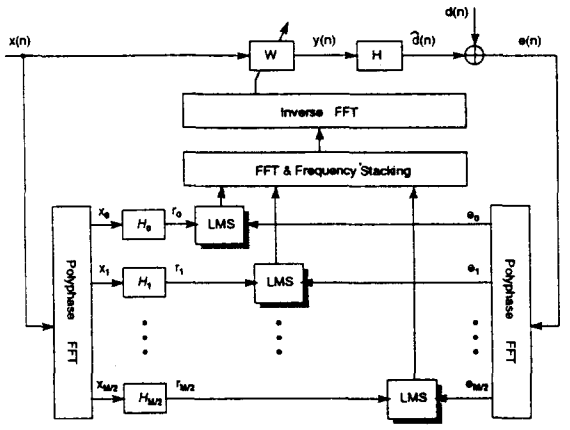

Fig. 2. Delayless subband ANC system with subband-decomposed secondary path transfer function.

The filtered reference signal is then obtained for each of subband with the subband-decomposed transfer functions.

A major advantage of this approach inherits from the reduction of computational complexity. Assuming that the secondary path transfer function is modeled as an Lth order FIR filter, L multiplications per sample are normally required to compensate for the distortion caused by the secondary path. However, with the same transfer function, the number of multiplications is reduced down to L/M by decomposing the transfer function into M subbands. Subband decomposition of the secondary path transfer function is accomplished in reverse order of the procedure for obtaining the wideband filter response from the adaptive weights of each subband filter. First, the L coefficients are transformed by L-point FFT's to obtain$L$ frequency components. Assuming the coefficients are real, only half of the M subbands need to be processed, corresponding to the positive frequency components of the wideband secondary path transfer function. Therefore, $L/2$ frequency components are appropriately decomposed into each of $M/2$ subbands. Finally, the $2L/M$ frequency components per each subband are transformed by an inverse FFT to obtain the $2L/M$ coefficients of the subband-decomposed transfer functions.

Fig. 2 shows the structure of the delayless subband ANC system with subband-decomposed secondary path transfer function. Using the structure presented in Fig. 2, the secondary path response can be adaptively estimated in the subband structure, rather than the wideband filter structure shown in Fig. 1. Fig. 3 shows the schematic diagram of the delayless subband ANC system comprising the on-line system identification filter implemented in each subband. Defining the coefficient vectors of the system identification filter for the mth subband as $\mathbf{c}_m(n)$ and $\mathbf{d}_m(n)$, they are updated to minimize the power of the error signal given by

$$\hat{e}_m(n) = e_m(n) - \mathbf{c}_m^H \mathbf{x}_m(n) - \mathbf{d}_m^H \mathbf{y}_m(n), \qquad (14)$$

where $\mathbf{y}_m(n)$ is the output of the mth subband adaptive filter. Now, the weight vector is updated using the complex NLMS algorithm to obtain the update equations given by

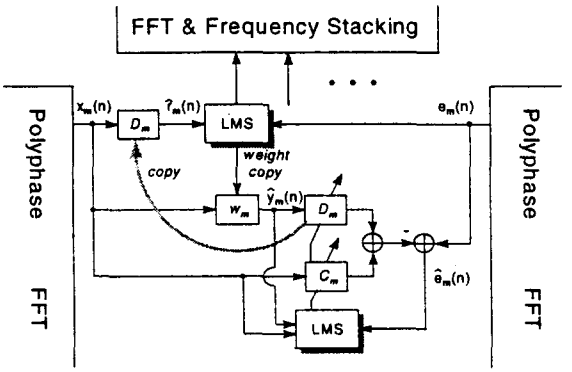

Fig. 3. Schematic diagram of the delayless subband ANC system comprising the on-line system identification filter in each subband.

$$\mathbf{c}_m(n+1) = \mathbf{c}_m(n) + \frac{\kappa}{\sigma_{x_m}^2(n) + \sigma_{y_m}^2(n)} \hat{e}_m(n)\mathbf{x}_m(n), \qquad (15)$$

$$\mathbf{d}_m(n+1) = \mathbf{d}_m(n) + \frac{\kappa}{\sigma_{x_m}^2(n) + \sigma_{y_m}^2(k)} \hat{e}_m(n)\mathbf{y}_m(n), \qquad (16)$$

$$\sigma_{x_m}^2(n) = (1-\kappa)\sigma_{x_m}^2(n-1) + \kappa|x_m(n)|^2, \qquad (17)$$

$$\sigma_{y_m}^2(n) = (1-\kappa)\sigma_{y_m}^2(n-1) + \kappa|y_m(n)|^2. \qquad (18)$$

Table 1 summarizes the number of multiplications per input sample for the on-line identification. In the wideband structure, $2L$ multiplications are needed for the coefficient update and another $2L$ multiplications are required to calculate $\hat{e}(n)$ for on-line system identification. When the system identification filter is implemented in subband as shown in Fig. 3, $8N/M$ multiplications are needed to calculate $\hat{y}_m(n)$, $8L/M$ multiplications are needed for coefficients update, and $16L/M$ multiplications are needed for the filter output computation. For example, with $N = 512$ for full band taps, $M = 32$ for subbands and $L = 256$ for the FIR filter coefficients for the secondary path identification, 1024 multiplications per input sample are needed for the wideband structure, but only 320 multiplications are needed for the subband structure. Thus, in this particular case the subband approach reduces the computational load for the system identification by a factor 3.

Table 1. Computational complexity comparison for the on-line system identification.

	procedure	multiplications
wideband	convolution	$2L$
	coefficient update	$2L$
subband	filter output	$8N/M$
	convolution	$8L/M * 2$
	coefficient update	$8L/M$

4. SIMULATION RESULTS

For simulations, an one-dimensional duct with length $a = 5.6m$ was assumed. A primary source is positioned at one end of the duct and the other end of the duct is closed with a rigid cap.

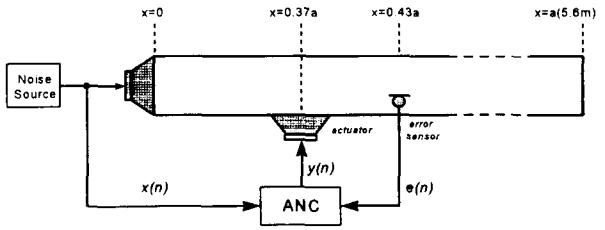

Fig. 4. Configuration of the simulation environment.

The control source driven by the adaptive filter is located at the position $0.34a$ and the error sensor providing the feedback error signal is located at the position $0.47a$ as shown in Fig. 4. The sampling frequency was 1000Hz.

The primary path and secondary path frequency responses were calculated from the modal model of the sound field [1]. The impulse response estimates were then computed from the frequency responses. The primary path was modeled as a 512-tap FIR filter and the secondary path was modeled as a 256-tap FIR filter. The reference signal was taken to be white noise through a band pass filter with a passband from 100 to 450Hz. Three harmonics (120, 240 and 360Hz) were added to the reference signal.

With the generated wideband signal, the performance of the presented algorithm was evaluated. As demonstrated in Fig. 5, almost the same performance can be obtained using the proposed approach. It should be noted that the minor difference between two approaches observed from Figs. 5 is accompanied by the decomposition error generated during the subband decomposition.

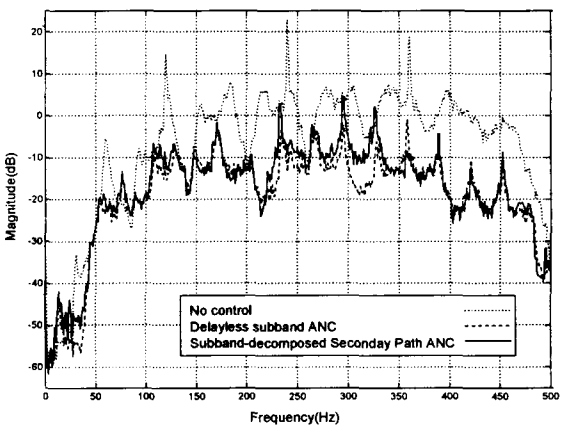

Fig. 5. Steady state power density spectrum.

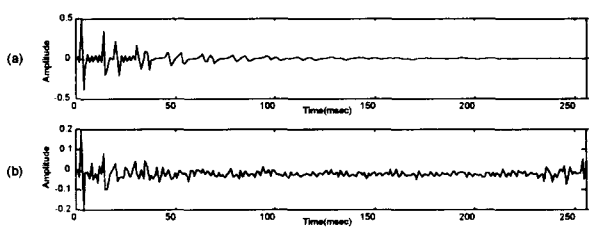

Fig. 6. (a) Impulse responses of the secondary path and (b) estimated impulse response of the secondary path for the subband approach shown in Fig.3.

Fig. 6 shows the impulse response of the secondary path and its estimate using the delayless subband approach described in Fig. 3.

Results demonstrate that the use of the delayless subband approach provides a reasonable estimate of the true impulse response. Also, it was observed that the convergence speed of the method presented was comparable to the wideband approach shown in Fig 1.

5. CONCLUSIONS

In this paper, a new active noise control algorithm based on a delayless subband adaptive filter architecture and an on-line system identification method implemented in the subband structure were presented.

In the new ANC algorithm, the filtered-x LMS algorithm is implemented in the subband structure with the secondary path transfer function that is decomposed into sets of subband functions. The secondary path transfer function is then adaptively estimated for each subband in decomposed form, so that the structure presented here has benefits in computational complexity that is reduced by a factor 3 compared with the wideband approach.

Simulation results were presented to confirm the efficiency of the new ANC algorithm and on-line system identification scheme presented in this paper.

REFERENCES

[1] P. A. Nelson and S. J. Elliott, *Active Control of Sound*, Academic Press, New York, 1992.

[2] B. Widrow and S. D. Stearns, *Adaptive Signal Processing*, Prentice-Hall, Englewood Cliffs, NJ, 1985.

[3] J. J. Shynk, "Frequency-domain and multirate adaptive filtering," *IEEE Signal Processing Mag.*, vol. 9, pp. 14-37, Jan.1992.

[4] D. R. Morgan and J. C. Thi, "A delayless subband adaptive filter architecture," *IEEE Transactions on Signal Processing*, vol. 43, No. 8, 1995.

[5] J. C. Burgess, "Active adaptive sound control in a duct: a computer simulation," *Journal of the Acoustic Society of America*, **70**, pp. 715-726, 1981.

[6] D. R. Morgan, "An analysis of multiple correaltion cancellation loops with a filter in the auxiliary path," *IEEE Transactions on Acoustics, Speech, Signal Processing*, **ASSP-28**, pp. 454-467, 1980.

[7] E. R. Ferrara, Jr., "Frequency-domain adaptive filtering," in *Adaptive Filters*, C. F. N. Cowan and P. M. Grant, Eds., Englewood Cliffs, NJ: Prentice-Hall, ch. 6, pp. 145-179, 1985.

[8] S. Haykin, *Adaptive Filter Theory*, Prentice-Hall, Englewood cliffs, NJ, 1992

[9] S. D. Sommerfeldt, "Multi-channel adaptive control of structural vibration," *Noise Control Engineering Journal*, **37** pp. 77-89, 1991.